Stem Cell Reports, Volume *9*

Supplemental Information

WT1 Is Necessary for the Proliferation and Migration of Cells of Renin Lineage Following Kidney Podocyte Depletion

Natalya V. Kaverina, Diana G. Eng, Andrea D. Largent, Ilse Daehn, Anthony Chang, Kenneth W. Gross, Jeffrey W. Pippin, Peter Hohenstein, and Stuart J. Shankland

Supplemental Figures

Figure S1

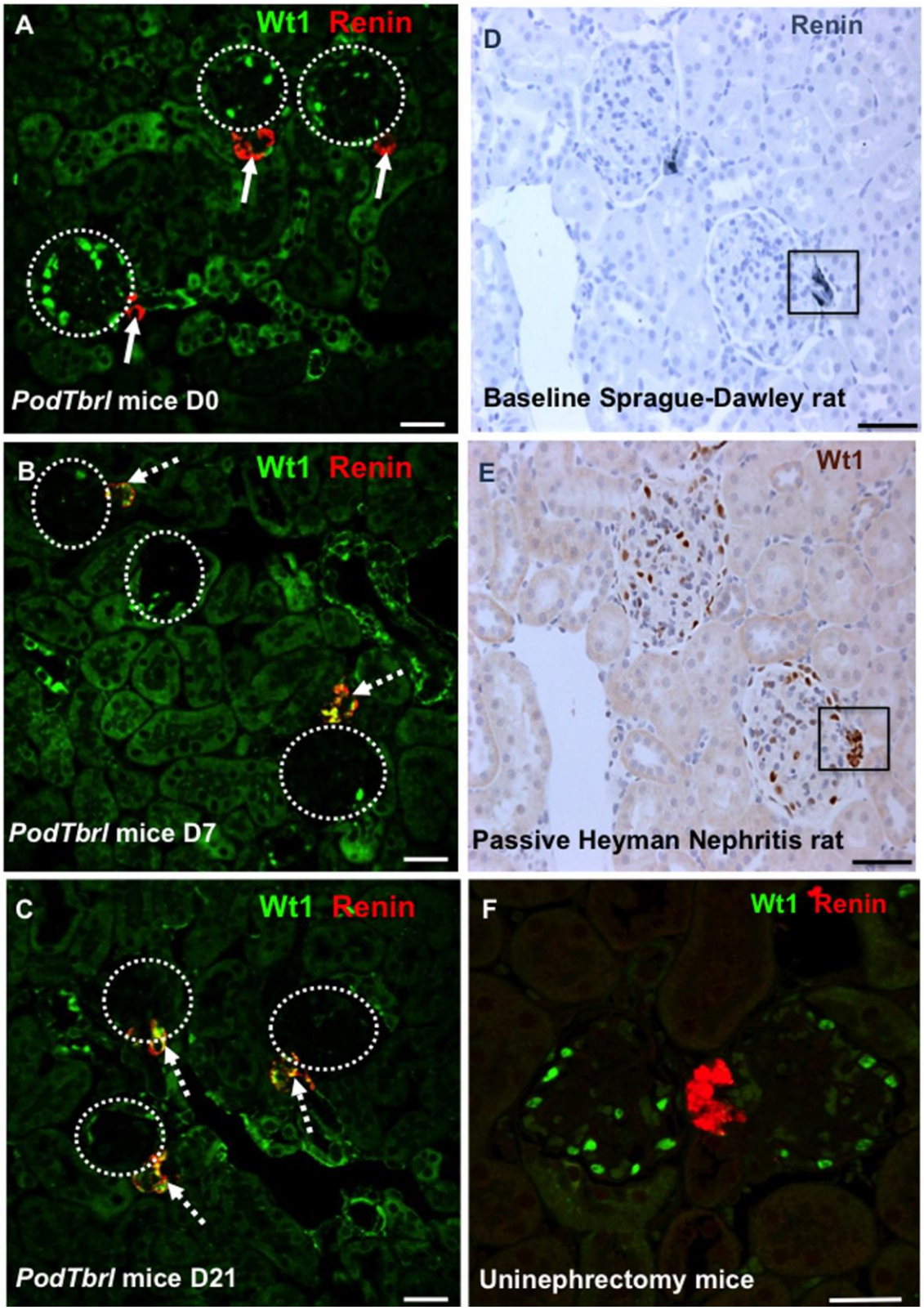

Figure S1: ***WT1 staining is increased in renin-expressing cells following podocyte depletion in podocyte TGFß-Receptor1 transgenic mice and the passive Heymann nephritis model, but not in the uninephrectomy model of glomerular hypertrophy.***

(A-C) *Podocyte TGFß-Receptor1 transgenic (PodTgfbr1) mice*: Representative two-color immunofluorescence double staining of WT1 (green) and Renin (red, solid arrow). The outline of glomeruli is shown with dashed circles. (**A**) At D0 in mice not given doxycycline, renin was confined to the juxta-glomerular compartment (JGC), and WT1 to glomeruli, hence there was no overlap. (**B**) Decreased glomerular WT1 staining represents marked podocyte depletion at D7 after doxycycline induction. WT1 staining is increased in renin-expressing cells (yellow color marked with dashed arrows). (**C**). At D21, podocyte depletion was persistent. WT1 staining merges with RFP cells in the JGC.

Scale bars represent 20μm.

(D, E) *PHN model of membranous nephropathy.* Two sequential kidney sections (4μm thick) were stained with renin (dark blue) and WT1 (brown) respectively. renin stained cells marked with solid boxes in the JGC (**D**) co-stain for WT1 (**E**). Scale bars represent 20μm.

(**F**) *Uninephrectomy model.* Double immunofluorescence shows that WT1 (green) and renin (red) do not colocalize (no yellow color) in this model where absolute podocyte number is unchanged. Scale bars represent 20μm.

Figure S2

Kaverina et al.

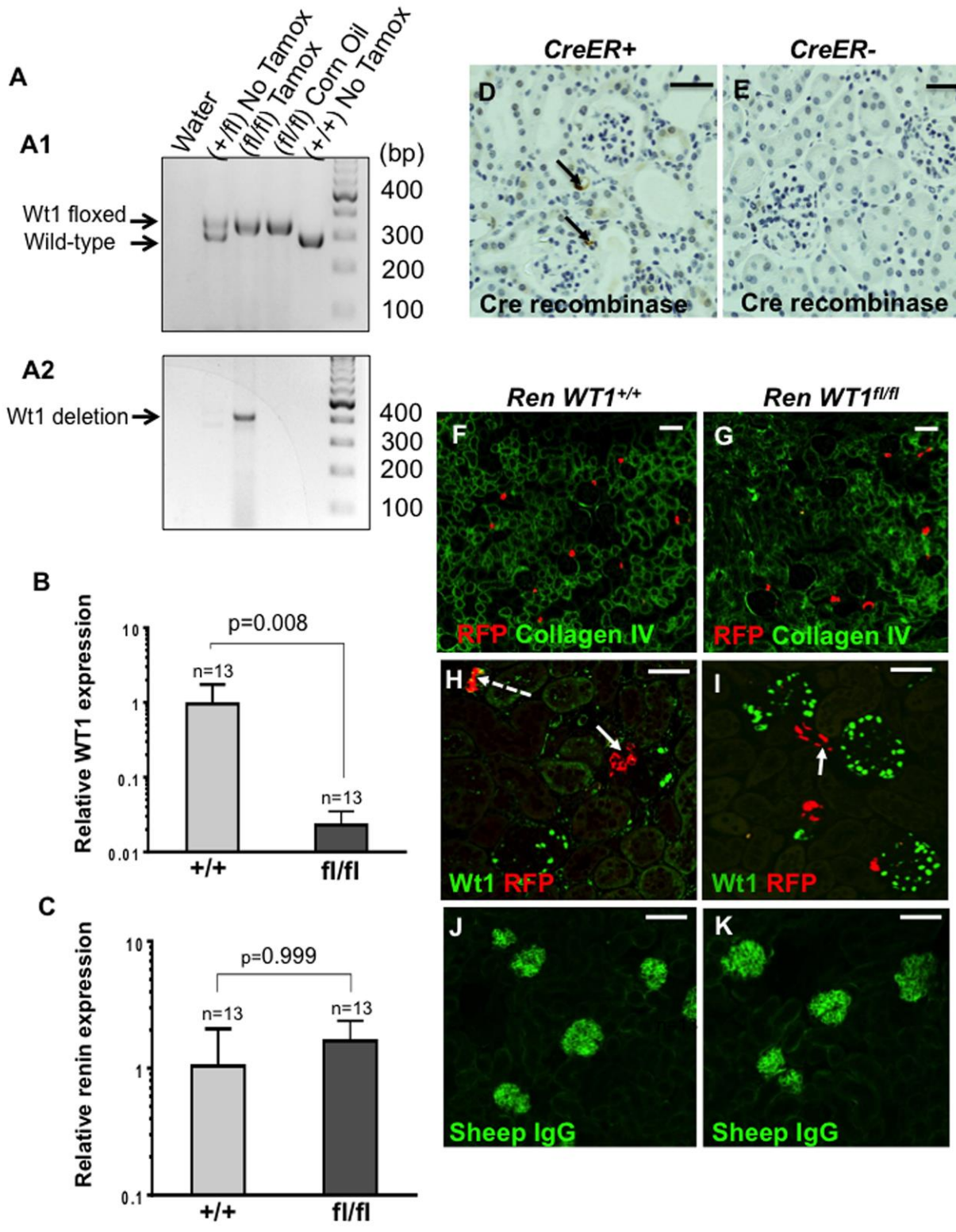

Figure S2: ***Characterization of RenWt1$^{+/+}$ and RenWt1$^{fl/fl}$ reporter mice*.**

(**A**) *Genotyping*: (**A1)**: Tail snip DNA was used for PCR to identify animals that carried CreER, and either the wildtype (327bp) or floxed Wt1 (300bp) alleles. DNA loaded from left to right includes no DNA (water), *RenWt1$^{+/fl}$* no tamoxifen (tamox), *RenWt1$^{fl/fl}$* administered tamox, *RenWt1$^{fl/fl}$* administered vehicle (corn oil), and *RenWt1$^{+/+}$* no tamox. (**A2**) DNA isolated from kidney cortex from the above animals underwent PCR to verify the Cre-mediated deletion of the floxed Wt1 (420bp) in *RenWt1$^{fl/fl}$* animals given tamox. As expected, animals not given tamoxifen did not show a flox deletion band.

(B, C) *Relative mRNA expression*: qPCR of mRNA from laser captured RFP positive cells in the juxta-glomerular compartment from *RenWt1$^{+/+}$* and *RenWt1$^{fl/fl}$* mice given tamox. (**B**) Relative Wt1 expression is significantly less in *RenWt1$^{fl/fl}$* animals. (**C**) There is no significant differences in renin mRNA in the same samples (n=13/per group)

(**D, E**) *Cre recombinase staining* is detected in the JGC of CreER positive animals (arrow), but not in cre negative animals as expected. Scale bars represent 20μm.

(**F, G**) *Reporting:* Collagen IV (green) was used to delineate glomeruli. Low power view shows that tdTomato reporter (red) was similar in *RenWt1$^{+/+}$* and *RenWt1$^{fl/fl}$* mice given tamoxifen. Scale bars represent 50μm.

(**H, I**) *WT1 staining:* In baseline *RenWt1$^{+/+}$* mice, WT1 staining (green) is co-expressed in less than 5% of RFP^{+} cells (red, solid arrows), creating a yellow color (dashed arrow). WT1 staining is not detected in RFP cells in *RenWt1$^{fl/fl}$* mice. Scale bars represent 20μm.

(**J, K**) *Sheep IgG staining*: used to determine deposition of the cytotopathic anti-podocyte antibody to induce podocyte loss, was similar in *RenWt1$^{+/+}$* and *RenWt1$^{fl/fl}$* mice. Scale bars represent 40μm.

Figure S3

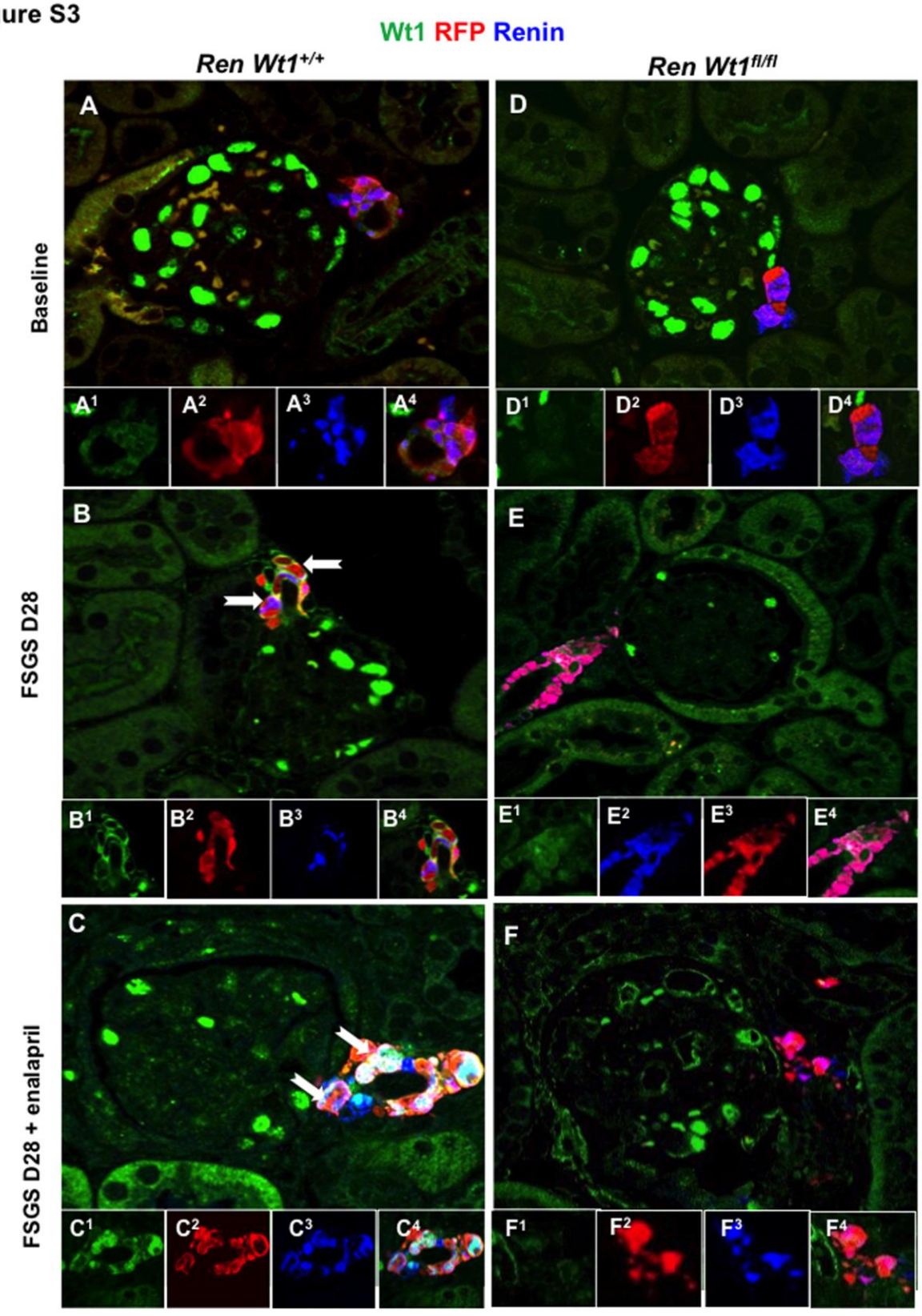
Wt1 RFP Renin
Ren Wt1+/+
Ren Wt1fl/fl
Baseline
FSGS D28
FSGS D28 + enalapril
A
A1
A2
A3
A4
D
D1
D2
D3
D4
B
B1
B2
B3
B4
E
E1
E2
E3
E4
C
C1
C2
C3
C4
F
F1
F2
F3
F4

Figure S3: ***Cells of renin lineage (CoRL) co-expressing renin and WT1 in RenWt1$^{+/+}$ mice following podocyte depletion in the cytotoxic anti-podocyte antibody model of FSGS.***

(**A-F**) Triple staining was performed with antibodies to WT1 (green), red fluorescent protein (RFP, red) and renin (blue) in *RenWt1$^{+/+}$* and *RenWt1$^{fl/fl}$* mice, and imaged using confocal microscopy. The larger pictures show the merge of all three colors; individual panels labeled 1-4 show individual colors for WT1, RFP, renin and their merge respectively. A merge of RFP, WT1 and renin creates a white color (**B, C**) (marked with solid arrows), and a merge of RFP and renin creates a purple color (**A, D-F**) (marked with dashed arrows).

In baseline *RenWt1$^{+/+}$* (**A**) and *RenWt1$^{fl/fl}$* (**D**) mice, WT1 staining was readily detected in podocytes; RFP and staining was restricted to the juxta-glomerulus compartment (JGC), and were indistinguishable at baseline. (**B**) At FSGS D28 in *RenWt1$^{+/+}$* mice, WT1 staining was detected in RFP^{+}CoRL in the JGC (marked with solid arrows). (**E**) WT1^{+}RFP^{+} staining was not detected in *RenWt1$^{fl/fl}$* mice at FSGS D28. The number of podocytes staining for WT1 was reduced in both strains at FSGS D28, but was more severe in diseased *RenWt1$^{fl/fl}$* mice. (**C**) Giving Enalapril to diseased *RenWt1$^{+/+}$* mice augmented WT1 expression in RFP+CoRL (marked with solid arrow), but not in diseased *RenWt1$^{fl/fl}$* mice (**F**).

Figure S4

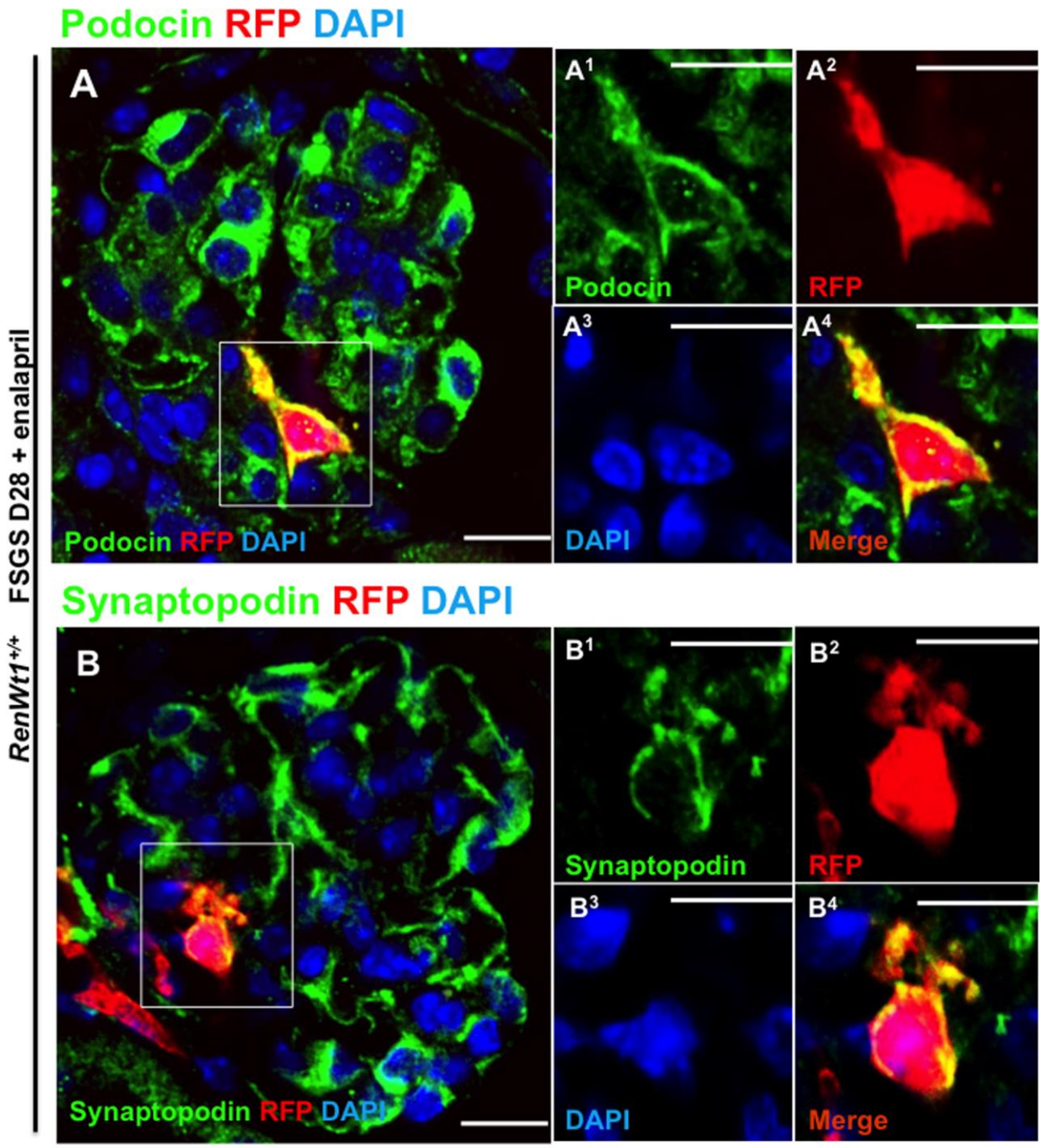
Podocin RFP DAPI
A
A1
A2
A3
A4
Podocin
RFP
DAPI
Merge
Podocin RFP DAPI
FSGS D28 + enalapril
RenWt1+/+
Synaptopodin RFP DAPI
B
B1
B2
B3
B4
Synaptopodin
RFP
DAPI
Merge
Synaptopodin RFP DAPI

Figure S4*: Cells of renin lineage (CoRL) begin to de novo express the podocyte markers in enalapril treated* RenWt1 $^{+/+}$ mice at D28 of FSGS following podocyte depletion.

(**A**) Representative image of three color staining for podocin (podocyte marker, green), RFP identifies td-Tomato-labeled CoRL, red) and DAPI.(nuclear, blue). (**A1-A4**) Insets show images of individual colors for podocin, RFP, DAPI and their merge respectively of CoRL in the glomerular tuft. Podocin (**A1**) co-localized with RFP+CoRL (**A2**) merging as yellow color (**A4**) with corresponding nuclear staining (**A3**)

(**B**) Representative image of three color staining for synaptopodin (podocyte marker, green), RFP identifies td-Tomato-labeled CoRL, red) and DAPI.(nuclear, blue). **(B1- B4**) Insets show images of individual colors for synaptopodin, RFP, DAPI and their merge respectively of CoRL in the glomerular tuft. Synaptopodin (**B1**) co-localized with RFP+CoRL (**B2**) merging as yellow color (**B4**) with corresponding nuclear staining (**B3**) Scale bars represent 20μm.

Figure S5

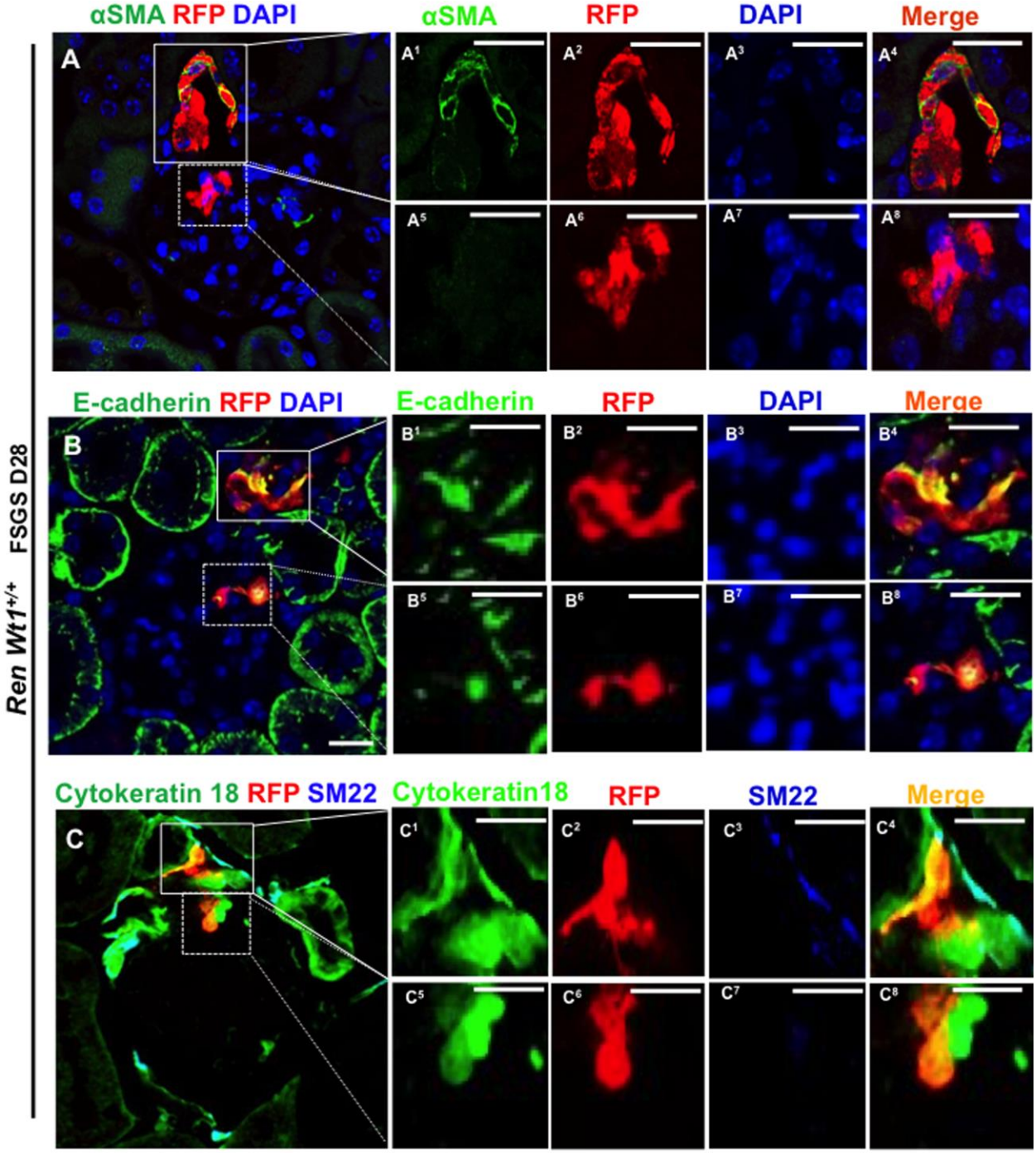
αSMA RFP DAPI
αSMA
RFP
DAPI
Merge
A
A1
A2
A3
A4
A5
A6
A7
A8
E-cadherin RFP DAPI
E-cadherin
RFP
DAPI
Merge
B
B1
B2
B3
B4
B5
B6
B7
B8
Cytokeratin 18 RFP SM22
Cytokeratin18
RFP
SM22
Merge
C
C1
C2
C3
C4
C5
C6
C7
C8
Ren Wt1+/+ FSGS D28

Figure S5*: Following podocyte depletion in the cytotoxic anti-podocyte antibody model, cells of renin lineage (CoRL) that migrate from the juxtaglomerular compartment (JGC) to the glomerulus de novo express epithelial markers, and no longer express mesenchymal markers.*

(**A**) *Loss of mesenchymal marker when CoRL migrates to glomerulus following podocyte depletion*. Confocal images shows three color staining for αSMA (mesenchymal marker, green), RFP (labeled CoRL, red) and DAPI (nuclear, blue). Solid box indicates the JGC, dashed box indicates CoRL in the glomerular tuft. Higher magnification views of individual stains labeled as superscripted panels 1-4. In the JGC, αSMA (**A1**) is constitutively expressed in RFP^+CoRL (**A2**), merging as a yellow/ orange color (**A4**) with corresponding nuclear staining (**A3**). In contrast, αSMA staining (**A5**) is not detected in a RFP+ cell in the glomerular tuft (**A6**), and thus no merge (**A8**).

(B) *De novo staining for an epithelial cell marker in the JGC persists when CoRL migrates to the glomerulus*. Confocal microscopy shows staining for E-cadherin (epithelial marker, green), RFP (CoRL, red) and DAPI (nuclear, blue) in the JGC (solid inset) and glomerular tuft (dashed inset) at D28. In the JGC, there is de novo staining for E-cadherin (green, **B1**) that co-localizes with RFP (**B2**), to create a merged yellow/orange color (**B4**). In the glomerulus, E-cadherin staining persists (**B5**) in an RFP^+ cell (**B6**) to create a yellow/orange color (**B8**).

(**C**) *In the glomerulus, a migrated CoRL loses mesenchymal markers while de novo expressing epithelial marker*. Confocal microscopy shows staining for SM22 (mesenchymal marker, blue), Cytokeratin 18 (epithelial marker, green) RFP (identifies CoRL, red). JGC and glomerular tuft shown with solid and dashed insets respectively. In the JGC following podocyte depletion, RFP^+ cells (**C2**) co-express cytokeratin 18 (**C1**) and SM22 (**C3**) to merge as a light blue color (**C4**). In the glomerulus, an RFP^+ cell (**C5**), co-expresses cytokeratin 18, but no longer expresses SM22, to create a yellow color (**C8**). Scale bars represent 20μm.

Figure S6

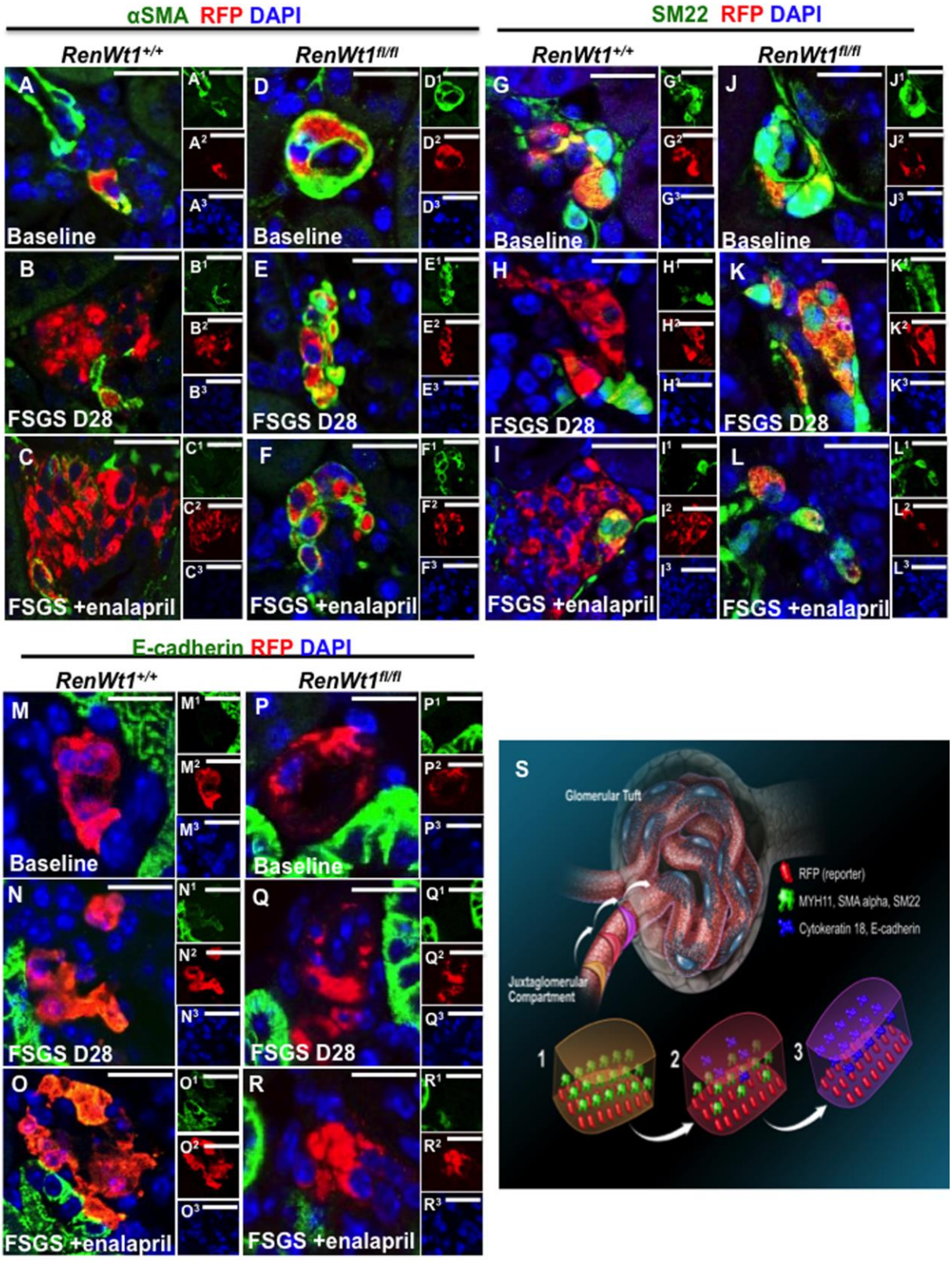
αSMA RFP DAPI
SM22 RFP DAPI
RenWt1+/+
RenWt1fl/fl
Baseline
FSGS D28
FSGS +enalapril
E-cadherin RFP DAPI
S
Glomerular Tuft
Juxtaglomerular Compartment
RFP (reporter)
MYH11, SMA alpha, SM22
Cytokeratin 18, E-cadherin
1
2
3

Figure S6: ***Following podocyte depletion, cells of renin lineage (CoRL) in the juxta-glomerular compartment (JGC) have reduced staining for mesenchymal markers, but increased staining for epithelial cells markers***.

(**A-F**) *Images are limited to the JGC, showing the mesenchymal marker αSMA (green) and RFP (red) co-staining with DAPI counterstain (blue). Individual insets labeled by superscript show individual stains. Scale bars represent 20μm.*

(**A-C**) *RenWt1*$^{+/+}$ mice. (**A**) At baseline, αSMA (**A1**) is readily detected in RFP cells (**A2**) in the JGC, merging to create a yellow color. (**B**) At D28 FSGS, αSMA staining is reduced (**B1**) in RFP cells (**B2**) that have increased in number. (**C**) At D28 with enalapril, αSMA staining (**C1**) is markedly reduced in RFP cells (**C2**), leading to very little if any merged color due to a decrease in staining of αSMA in RFP cells.

(**D-F**) *RenWt1*$^{fl/fl}$ mice. (**D**) At baseline, αSMA staining (**D1**) overlaps with RFP (**D2**) to create a yellow color in cells of the JGC. (**E, F**) At D28 FSGS and D28 with enalapril, αSMA staining (**E1, F1**) remains unchanged from baseline in RFP cells (**E2, F2**).

(**G-L**) *Co-staining for the mesenchymal marker SM22 (green) and RFP (red) in cells of the JGC, counterstained with DAPI (blue).* Scale bars represent 20μm. (**G-I**) *RenWt*$^{+/+}$ mice. (**G**) At baseline, SM22 staining (**G1**) is abundant in RFP cells (**G2**), merging to create a yellow color. (**H**) At FSGS D28, SM22 staining decreases (**H1**) in RFP cells (**H2**), leading to less merge evidenced by less yellow color. (**I**) At D28 plus enalapril, SM22 staining decreases markedly (**I1**), although the number of RFP cells (**I2**) increases.

(**J-L**) *RenWt1*$^{fl/fl}$ mice. SM22 staining is readily detected in RFP cells in the JGC creating a yellow color at baseline (**J**), which is unchanged at D28 FSGS (**K**) and D28 FSGS with Enalapril (**L**).

(**M-R**) *Co-staining for the epithelial cell marker E-cadherin (green) and RFP (red) in cells of the JGC, counterstained with DAPI (blue).* Scale bars represent 20μm. (**M-O**) *RenWt*$^{+/+}$ mice. (**M**) At baseline, E-cadherin staining (**M1**) is detected in the tubules, but not in RFP cells (**M2**) in the JGC. (**N**) At D28 FSGS, de novo E-cadherin staining (**N1**) is detected in RFP cells (**N2**), creating a yellow color. (**O**) In FSGS mice given enalapril, de novo E-cadherin staining is abundant (**O1**) in RFP cells (**O2**).

(**P-R**) *RenWt1*$^{fl/fl}$ mice. The epithelial marker E-cadherin is not expressed in RFP cells at baseline (**P**), D28 FSGS (**Q**) and D28 enalapril treated FSGS mice (**R**).

(**S**) *Schema depicting CoRL mesenchymal-to-epithelial transition in Wt1 wildtype mice with FSGS*

Within the juxtaglomerular compartment, 1.) demonstrates the expression of the tdTomato reporter, detected by an antibody to RFP (indicated by the red bodies) and mesychmemal markers αSMA, MYH11, SM22 (indicated by the green bodies) 2.) Following podocyte depletion, RFP is maintained, however the mesenchymal makers decrease, as epithelial markers (indicated by the blue bodies) begin to increase. 3.) As MET progresses, RFP continues to be maintained, while the mesenchymal markers are absent and epithelial markers are expressed. Cells that migrate to glomerular tuft undergo to MET-like changes.

Figure S7

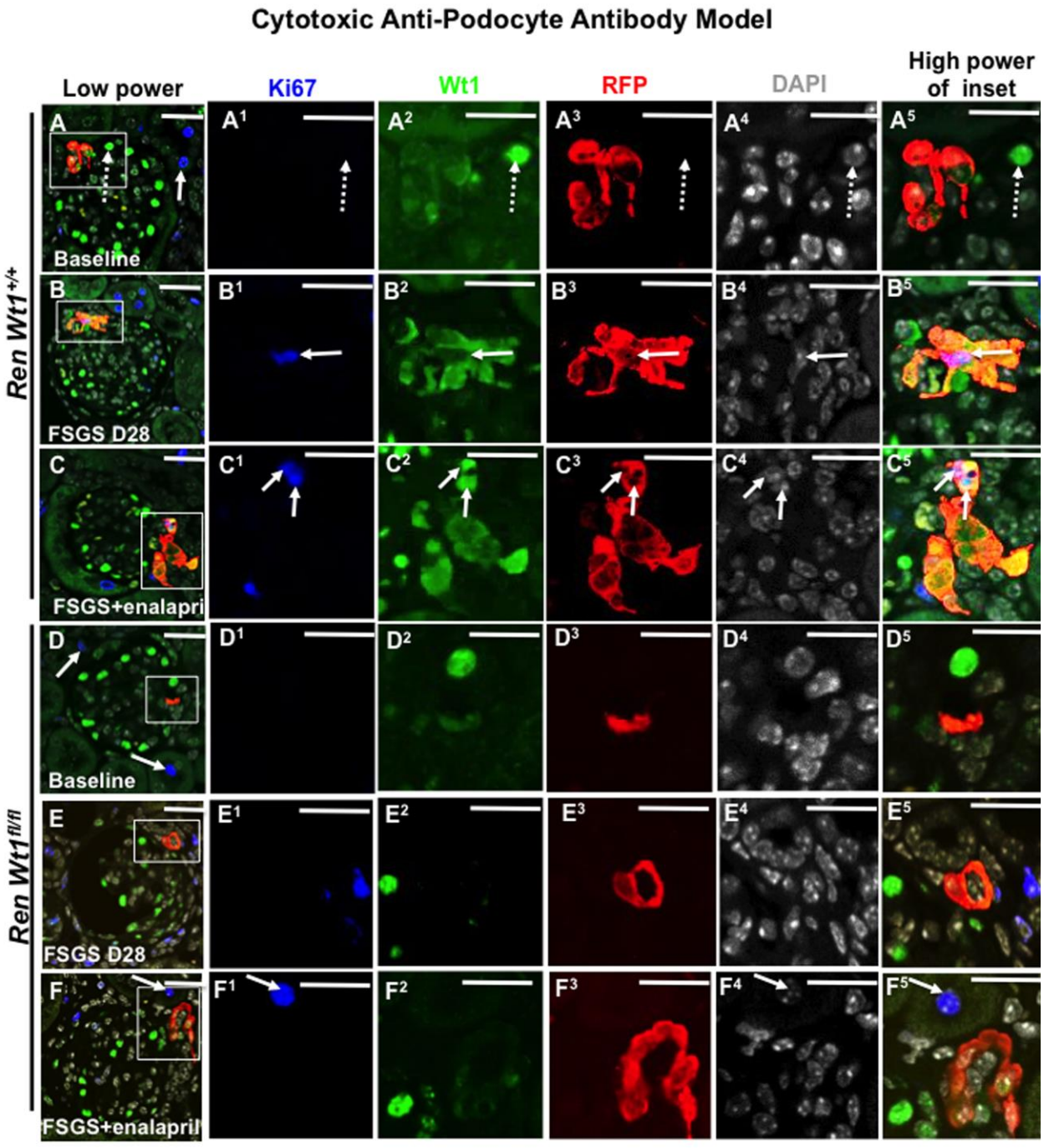
Cytotoxic Anti-Podocyte Antibody Model
Low power
Ki67
Wt1
RFP
DAPI
High power of inset
Ren Wt1+/+
Ren Wt1fl/fl
Baseline
FSGS D28
FSGS+enalapril
Baseline
FSGS D28
FSGS+enalapril

Figure S7: ***Following podocyte depletion in the cytotoxic anti-podocyte antibody model of FSGS, Ki67 is detected in WT1 stained cells of renin lineage.***

Confocal images of Ki67 (blue), WT1 (green), RFP (red) and DAPI (grey). Insets show the JGC, and the individual antibody panels from the inset are shown as enlarged pictures.

(**A-C**) *RenWt1*$^{+/+}$ mice. (**A**) At baseline, Ki67 (**A1**) is not detected in the JGC, but is detected in neighboring tubules (solid arrow). WT1 staining (**A2**) is not detected in RFP cells (**A3**), but is positive in neighboring podocyte (dashed arrow). (**B**) At D28, Ki67 (**B1**, solid arrow) is detected in WT1 stained cells (**B2**) that co-localizes with RFP (**B3**). The triple merge (Ki67, WT1, RFP) creates a white/purple color (arrow), and the merge of WT1 and RFP creates a yellow color. (**C**) In FSGS mice given enalapril, the number of Ki67 cells (**C1**) increased in WT1 stained cells (**C2**) that overlap with RFP (**C3**). The merge of 3 colors creates a white/purple color (arrow), and the increase in yellow reflects increased WT1 in RFP cells.

(**D-F**) *RenWt1fl/fl* mice. (**D**) At baseline, Ki67 cells are detected in tubules (arrow), but not in the JGC (**D1**). WT1 (**D2**) is not present in RFP^{+} cells (**D3**). (**E**) At D28, neither Ki67 (**E1**) nor WT1 (**E2**) are detected in RFP cells (**E3**). (**F**) In FSGS mice given enalapril, Ki67 was restricted to the tubules (arrow) but not the JGC (**F1**). WT1 (**F2**) is not detected in RFP cells (**F3**). Scale bars represent 20 μm.

Supplemental Experimental Procedures

RenCreER tdTomato Wt1$^{fl/fl}$ reporter mice

Ren1cCreERxRs-tdTomato-R mouse (described previously) (Pippin et al., 2013) were crossed with a *Wt1* conditional knockout mouse strain (Wt1$^{fl/fl}$) (Martinez-Estrada et al., 2010). *Wt1* was inactivated in *RenCreER tdTomato Wt1$^{fl/fl}$* mice (abbreviated *RenWt1)* by administration of 100 mg/kg tamoxifen on four occasions. The genotype of animals was identified by PCR. PCR conditions and primer sequences have been described previously (Martinez-Estrada et al., 2010). Mice were then given a tamoxifen washout period of 4 weeks, to allow it to complete exit the body and make certain no new Ren1c-creER expressing cells were labeled prior to the initiation of experiments.

Survival kidney biopsies were performed to ensure and assess CoRL labeling. Briefly, mice were anesthetized with isoflurane, and checked for depth of anesthesia via toe pinch. When the mouse is no longer responsive to external stimuli, hair is removed from the area above the kidney using clippers. Skin around the site of the incision will be disinfected using aseptic technique, on a sterile field above a circulating water heat pad. An incision is made on the flank about (1.0 cm behind the ribs and about 0.5cm below the major hack muscles in mice). A sterile drape with an opening exposing the surgical site is placed over the incision site. The kidney, renal artery and renal vein are exposed through the incision. A micro-vessel clamp is placed on the renal artery and vein to reduce blood flow during biopsy (duration 1 minute). A small piece of kidney (0.4 x 0.2mm) is removed with a sharp scalpel blade. Immediately following, a piece of sterile Gelfoam (hemostatic gelatin sponge) is placed on the kidney to prevent bleeding at the biopsy site. The micro-vessel clamp is removed and kidney is checked to make certain there is no bleeding before repositioning back into the body cavity. The peritoneum and muscle will be sutured together with polyglycolic acid absorbable sutures and the skin opening closed with non-absorbable sutures or surgical clips. The

wound will be cleaned again. The mouse will be allowed to recover, under observation, on a heated pad until ambulatory. Buprenorphine is given 30 minutes pre surgery and given post-surgery to maintain pain management for at least 72 hours *RenWt1*$^{fl/fl}$ and *RenWt1*$^{+/+}$ were housed in the animal care facility of the University of Washington under specific pathogen-free conditions with food and water available ad libitum. These studies were reviewed and approved by the University of Washington Institutional Animal Care and Use Committee (2968-04)

Experimental models of glomerular disease accompanied by podocyte depletion

The following experimental models of podocyte depletion were used for study:

(i) Experimental FSGS in *RenWt1*$^{fl/fl}$ and *RenWt1*$^{+/+}$ mice: Podocyte number was abruptly depleted in *RenWt1*$^{fl/fl}$ and *RenWt1*$^{+/+}$ mice with a cytotoxic sheep anti-glomerular antibody as previously described (Kaverina et al., 2016, Lichtnekert et al., 2016). On day three of disease, when podocyte number is decreased by 30-40% from baseline, mice were randomized into two groups; group 1 received drinking water (the vehicle for Enalapril); group 2 received the ACE-inhibitor Enalapril (75 mg/ml), refreshed weekly. Mice were sacrificed on day 28. Urine was collected at baseline, day7, day 14 and day 28. BrdU (5-bromo-2- deoxyuridine and 5-fluoro-2'-deoxyuridine) was administered to quantitate cell proliferation as previously described (Kaverina et al., 2016).

(ii) Podocyte TGFß - Receptor1 transgenic (*PodTgfbr1*) mice: Podocyte number is depleted in PodTgfbr1 by doxycyline induced TGFβR1 signaling specifically in podocytes. Progressive podocyte apoptosis leads to ∼25% depletion in podocytes by day 7 and ∼40% by day 14, accompanied by segmental and global glomerulosclerosis (Daehn et al., 2014).

(iii) Passive Heymann nephritis (PHN) model of membranous nephropathy: The (PHN) model of experimental membranous nephropathy was induced in male Sprague-Dawley rats (Charles River, Wilmington, MA) weighing 180 to 200 g by intraperitoneal injection of sheep antibody to Fx1A (5 mL/kg body weight) as previously described (Ohse et al., 2010) . Podocyte depletion has been characterized in the PHN model (Petermann et al., 2003).

(iv) Uninephrectomy model: The uninephrectomy model served as a negative control for podocyte depletion (Pippin et al., 2015). Following tamoxifen administration and washout, in *RenWt1*$^{+/+}$ as described above, kidney mass was reduced surgically. Mice were anesthetized, the left renal artery and vein were exposed through an incision and ligated with silk suture. The kidney capsule was removed from the kidney and remained along with the adrenal gland, while the left kidney itself was removed. Following recovery, the remaining right kidney was removed 12 weeks later.

BrdU labeling of mice to assess proliferation

BrdU (5-bromo-2- deoxyuridine and 5-fluoro-2'-deoxyuridine) was administered to quantitate cell proliferation. All animal groups, received BrdU 10µl per gram body weight (BrdU-Amersham Cell Proliferation Labeling Reagent, GE Healthcare Life Sciences, Pittsburgh, PA, RPN 202). Administration began the day after the last dose of anti-glomerular antibody was administered and was administered every 48 hours until sacrifice.

Laser Capture Microscopy (LCM) and quantitative reverse transcriptase polymerase chain reaction (qRTPCR) To ensure Wt1 deletion from CoRL, frozen kidney sections (10µm) from *RenWt1*$^{+/+}$ and *RenWt1*$^{fl/fl}$ samples were placed on positively charged glass slides. To isolate cells of renin lineage LCM was then performed as described (Tretiakova et al., 2011) with the Leica Laser Microdissection Systems LMD6500 & LMD7000 (Leica Microsystems Inc., Buffalo Grove, IL). An average of 100 to 300 cells per LCM cap were obtained from each sample and immediately subjected to complementary DNA (cDNA) synthesis and PCR. Total RNA was extracted using RNeasy Mini Kit (QIAGEN, Germantown, MD). Complementary DNA (cDNA) was synthesized using iScript cDNA Synthesis Kit (Bio-Rad, Hercules, CA). qRT-PCR assay was performed using an 7900 HT Sequence Detection System (Applied Biosystems, Foster City, CA) and iTaq SYBR Green Supermix with ROX (Bio-Rad, Hercules, CA). The thermocycling conditions consisted of denaturation at 95°C for 2.5 minutes, followed by cycles of 95°C for 15 seconds and amplification at 58°C for 30 seconds. A single PCR product of the expected size was verified by agarose gel electrophoresis. The primer sequences used were as follows: 18S forward TAGAGGGACAAGTGGCGTTC, 18S reverse CGCTGAGCCAGTCAGTGT, Ren1 forward GGAGGAAGTGTTCTCTGTCTACTACA, Ren1 reverse GCTACCTCCTAGCACCACCTC, Wt1 forward CCAGCTCAGTGAAATGGACA, Wt1 reverse CTGTACTGGGCACCACAGAG (Figure S1C).

Immunoperoxidase staining

Formalin fixed paraffin embedded mouse kidney sections (4µm thick) were deparaffinized in Histoclear, rehydrated in graded alcohol, and washed in phosphate buffered saline. The sections were boiled in 10mM citric acid buffer pH 6.0. and cooled for 30 minutes. Next, endogenous peroxidase activity was quenched with 3% hydrogen peroxidase solution and to block nonspecific reactions, sections were immersed in 5% milk solution for 20 minutes at room temperature. The following primary antibodies were applied on murine tissue: rabbit anti-p57 (Santa Cruz Biotechnology, Santa Cruz, CA, USA, sc-56341), rabbit anti-Cre-recombinase (Cell Signaling Technology, Danvers, MA, USA, 15036P). A horseradish peroxidase conjugated anti-rabbit polymer (Jackson Immunoresearch Laboratories, West, PA, USA, 111-001-003) was used to detect the primary antibodies. Sections were incubated with diaminobenzidine as a chromogen for 5 minutes, washed in water, and counterstained with hematoxylin. In some cases, Periodic acid Schiff's (PAS) staining was performed as a counterstain. Slides were dehydrated in ethanol and mounted with Histomount. Reactivity was judged positive only when distinct nuclear (p57) or cytoplasmic (anti-Cre-recombinase) staining was identified.

Multicolor immunofluorescent staining

Paraffin embedded mouse kidney sections (4µm thick) sections were used for staining. Deparaffinization, antigen retrieval and Avidin/Biotin blocking was performed as previously described (Lichtnekert et al., 2016). To identify podocytes, we used the following primary antibodies: rabbit anti-WT1 (Spring Bioscience, Pleasanton, CA, USA, E3990), rabbit anti-Podocin (Abcam, Cambridge, MA, USA, ab50339), mouse antibody to synaptopodin (Fitzgerald Industries International. Inc., Concord, MA, USA,10R-S125a). The appropriate biotinylated secondary antibody (Vector Laboratories) was applied followed by Streptavidin, AlexaFluor 488 conjugate (Life Technologies

- Molecular Probes, Grand Island, NY, USA, S-32354). To demarcate the glomerular compartment we stained slides with collagen IV (Southern Biotechnology, Birmingham, AL, USA, 1340-08), followed by Alexa647 conjugated donkey anti-rabbit IgG (Jackson ImmunoResearch Laboratories, West Grove, PA, USA, 711-605). Biotinylated anti-renin antibody (Innovative Research Novi, ISASPREN-GF-BIO), followed by Alexa 594 conjugated streptavidin (Life Technologies, S-32356) was applied to detect renin expression. To identify CoRL we used anti-RFP antibody (Dylite 594 conjugated RFP, Rockland Immunochemicals for Research, PA, 600-401-379). For all staining, omission of the primary antibody served as a negative control.

Immunostaining of CoRL and MET-markers

Paraffin embedded kidney sections (4μm) were used for staining. After performing deparaffinization, antigen retrieval and Avidin/Biotin blocking was performed as previously described (Lichtnekert et al., 2016). Antibodies were used to detect the following mesenchymal markers: αSMA (Sigma, Saint Louis, MI, USA, A2547), MYH11 (Abcam, Cambridge, MA, USA, ab53219), SM22 (Abcam, Cambridge, MA, USA, ab28811), NG2 (EMD Millipore Massachusetts, USA, AB5320). To identify epithelial cells, we used antibodies to the following markers: cytokeratin 18 (Bioss, Woburn, MA, USA, bs-2043R), E-cadherin (Cell Signaling, Danvers, MA, USA, 3195). Staining was detected with biotinylated mouse anti-rabbit IgG (Jackson ImmunoResearch) and visualized with Alexa488 conjugated streptavidin (Life Technologies). To prevent nonspecific staining for the primary antibodies from the same species pre-incubation with ChromePure rabbit IgG, Fab fragment (1:25;Jackson ImmunoResearch Laboratories, West Grove, PA,USA, 111-007) was followed by rabbit IgG Fab incubation (1:25;Jackson ImmunoResearch Laboratories, 111-003).
To identify CoRL, anti-RFP antibody (Dylite 594 conjugated RFP, Rockland Immunochemicals for Research, PA, 600-401-379) was used.

Triple staining of CoRL, WT1 and markers of proliferation

In order to check for proliferation of CoRL in experimental FSGS, we used the following antibodies: mouse anti-BrdU (Biocare Medical, Concord, UK, ACR3042) or rabbit anti-Ki67 (Abcam, Cambridge, MA, USA, ab15580) followed by appropriate biotinylated secondary antibody (Vector Laboratories). The signal was amplified by incubation with streptavidin conjugated with Alexa Fluor 647 (Invitrogen, Grand Island, NY, USA). To detect CoRL, anti-RFP antibody (Dylite 594 conjugated RFP, Rockland Immunochemicals for Research, PA, 600-401-379) was applied. To detect expression of WT1 we used primary rabbit anti-WT1 (Spring Bioscience, Pleasanton, CA, USA, E3990), followed by Alexa488 conjugated donkey anti-rabbit IgG (Jackson ImmunoResearch Laboratories, West Grove, PA, USA, 711-545).

.

Urine Collection, Urine Albumin Assay, Urine Creatinine Assay

Spot urine was collected at baseline, day 7, day 14 and day 28. Urine albumin was measured by radial immunodiffusion assay. Rabbit anti-mouse albumin antibody at 1:75 dilution (Accurate Chemical, Westbury, NY) and 4% rabbit serum (Pel-Freez, Rogers, AR) were incorporated into a thin layer of 1.5% type I, low EEO agarose

gel (Sigma-Aldrich) in 0.5 M veronal buffer, poured into Integrid 100x15 mm square petri dish on a leveling platform (VWR, West Chester, PA). Urine was placed in a well cut into the agar layer. As the antigens diffuse from the well, only the specific antigen (albumin) reacted with its antibody in the agar. The reaction formed a halo of precipitation around the well. A measurement of the halo after it had reached maximal size was related directly to antigen concentration, with reference made to a calibration curve prepared from known concentrations of purified fraction V mouse albumin standards (MP Biomedicals, Irvine, CA) tested under identical conditions. Creatinine was measured in the urine via a colorimetric assay according to the manufacturers instructions (Cayman Chemical, Ann Arbor, MI) and an albumin to creatinine ratio was calculated.

Confocal Microscopy

Images were obtained on Leica TCS SPE II laser scanning confocal microscope. Multi-color immunofluorescent images were collected at 200x and 400x magnification and a high 1.2 NA oil-immersion objective. Images were acquired in original Tagged Image Format File, with a bit depth of 15, no binning, and a total size of 512×512 pixels with each pixel corresponding to 0.27 μm. Each antibody staining was adjusted for background correction. Appropriate single stained controls were used with each antibody to check that there was no fluorochrome cross-bleeding.

Human biopsies of glomerular disease

In order to determine if the expression pattern for WT1 in renin expressing cells seen under experimental conditions was recapitulated in human disease, paraffin-embedded kidney biopsies from patients with FSGS, not otherwise specified (n=10) and Membranous nephropathy (n=10) were obtained from the University of Chicago. Normal human kidney paraffin-embedded sections were used as controls. The study protocol was approved by the University of Chicago Institutional Review Board. For double immunostaining of WT1 and renin, 4μm thick kidney sections were stained with immunofluorescent antibodies against WT1 (Spring Bioscience, Pleasanton, CA, USA) followed by Alexa488 conjugated donkey anti-rabbit IgG (Jackson ImmunoResearch Laboratories, West Grove, PA, USA) and biotinylated anti-renin antibody (LifeSpan Bioscience, Seattle, WA, USA), followed by Alexa 594 conjugated streptavidin (Life Technologies). Appropriate single stained controls were used with each antibody to ensure no fluorochrome cross-reactivity; omitting the primary antibodies served as negative controls.

Supplemental References

Daehn, I., G. Casalena, T. Zhang, S. Shi, F. Fenninger, N. Barasch, L. Yu, V. D'Agati, D. Schlondorff, W. Kriz, B. Haraldsson and E. P. Bottinger (2014). Endothelial mitochondrial oxidative stress determines podocyte depletion in segmental glomerulosclerosis. J Clin Invest 124, 1608-1621. Kaverina, N. V., D. G. Eng, R. R. Schneider, J. W. Pippin and S. J. Shankland (2016). Partial podocyte replenishment in experimental FSGS derives from nonpodocyte sources. Am J Physiol Renal Physiol 310, F1397-1413. Lichtnekert, J., N. V. Kaverina, D. G. Eng, K. W. Gross, J. N. Kutz, J. W. Pippin and S. J. Shankland (2016). ReninAngiotensin-Aldosterone System Inhibition Increases

Podocyte Derivation from Cells of Renin Lineage. J Am Soc Nephrol. Martinez-Estrada, O. M., L. A. Lettice, A. Essafi, J. A. Guadix, J. Slight, V. Velecela, E. Hall, J. Reichmann, P. S. Devenney, P. Hohenstein, N. Hosen, R. E. Hill, R. Munoz-Chapuli and N. D. Hastie (2010). WT1 is required for cardiovascular progenitor cell formation through transcriptional control of Snail and E-cadherin. Nat Genet 42, 8993. Ohse, T., M. R. Vaughan, J. B. Kopp, R. D. Krofft, C. B. Marshall, A. M. Chang, K. L. Hudkins, C. E. Alpers, J. W. Pippin and S. J. Shankland (2010). De novo expression of podocyte proteins in parietal epithelial cells during experimental glomerular disease. Am J Physiol Renal Physiol 298, F702-711. Petermann, A. T., R. Krofft, M. Blonski, K. Hiromura, M. Vaughn, R. Pichler, S. Griffin, T. Wada, J. Pippin, R. Durvasula and S. J. Shankland (2003). Podocytes that detach in experimental membranous nephropathy are viable. Kidney Int 64, 1222-1231. Pippin, J. W., N. V. Kaverina, D. G. Eng, R. D. Krofft, S. T. Glenn, J. S. Duffield, K. W. Gross and S. J. Shankland (2015). Cells of renin lineage are adult pluripotent progenitors in experimental glomerular disease. Am J Physiol Renal Physiol 309, F341-358. Pippin, J. W., M. A. Sparks, S. T. Glenn, S. Buitrago, T. M. Coffman, J. S. Duffield, K. W. Gross and S. J. Shankland (2013). Cells of renin lineage are progenitors of podocytes and parietal epithelial cells in experimental glomerular disease. Am J Pathol 183, 542-557. Tretiakova, M. and J. Hart (2011). Laser microdissection for gene expression study of hepatocellular carcinomas arising in cirrhotic and non-cirrhotic livers. Methods Mol Biol 755, 233-244. Zhang, J., D. Yanez, A. Floege, J. Lichtnekert, R. D. Krofft, Z. H. Liu, J. W. Pippin and S. J. Shankland (2015). ACEinhibition increases podocyte number in experimental glomerular disease independent of proliferation. J Renin Angiotensin Aldosterone Syst 16, 234-248.